



Performance-based multi-objective collaborative optimization of steel frames with fuse-oriented buckling-restrained braces

Xiang Tu¹ · Zheng He^{1,2} · Guohui Huang³

Received: 27 February 2019 / Revised: 11 June 2019 / Accepted: 18 July 2019 / Published online: 5 August 2019
© Springer-Verlag GmbH Germany, part of Springer Nature 2019

Abstract

A multi-objective collaborative optimal design procedure for steel frames equipped with buckling-restrained braces (BRBs) is proposed under the framework of performance-based seismic design (PBSD) in order to minimize the damage of the primary structure as well as the material cost. For this purpose, a so-called BRB energy dissipation ratio is defined and introduced in the optimization to characterize the involvement of fuse-type BRBs in hysteretic energy dissipation in building stories. Three groups of constraints obtained from the rules on geometrical and conceptual design, the requirements regarding strength and stability, and the PBSD-based story drift limits are considered. To address the discrete-continuous hybrid design variables, a hybrid coding scheme is proposed to modify the non-dominated sorting genetic algorithm II (NSGA-II). The rationality of the proposed procedure is demonstrated by a case study on a seven-story planar steel frame with BRBs. The demonstration indicates that the proposed optimization procedure can make BRBs play the role of a structural fuse successfully in steel frames. The BRB energy dissipation ratios of case C are distributed nearly uniformly along the structural height. The weak-beam-strong-column design principle can be satisfactorily achieved through the maximization of the story BRB energy dissipation ratios. Additionally, the modified hybrid coding NSGA-II algorithm is computationally efficient and stable.

Keywords Collaborative optimization · BRBF · NSGA-II · Energy dissipation ratio · Performance-based seismic design · Hybrid coding

1 Introduction

Due to their excellent hysteretic behavior, buckling-restrained braces (BRBs) have become more popular than ever in earthquake-resistant structures (Watanabe et al. 1988; Uang and Nakashima 2004). They have been proven to be a very efficient way to place BRBs in those structures for seismic retrofitting. For steel frames with BRBs (BRBFs), the seismic demand on the primary steel frame can be

significantly reduced by migrating any damage to secondary BRBs. In view of the relatively complex composition and manufacturing process, it is not economically acceptable to use BRBs extensively as an energy dissipation device. Thus, the economic benefit is a key factor that affects the usage of BRBs. In addition, as a special structural energy-absorbing device, BRBs are designed to yield during moderate and severe earthquakes to dissipate the energy absorbed by structural vibration. The more energy dissipated by the BRBs, the more likely the structure will remain safe when excited with strong earthquakes. As a result, the damage development within structural components becomes more controllable if a significant portion of the hysteretic energy can be dissipated by well-placed BRBs.

To reduce the damage to main structures in severe earthquakes, an appropriate structural design method must be adopted to make full use of the energy dissipation capacity of the BRBs. The traditional strength-based seismic design (SBSD) method is incapable of predicting inelastic behavior of BRBFs. To this end, performance-based seismic design (PBSD) methods have been widely applied, among which

Responsible Editor: Pingfeng Wang

✉ Zheng He
hezhen@dlut.edu.cn

¹ Department of Civil Engineering, Dalian University of Technology, Dalian 116024, China

² State Key Laboratory of Coastal and Offshore Engineering, Dalian University of Technology, Dalian 116024, China

³ China Machinery International Engineering Design & Research Institute Co., Ltd, Changsha 410007, China

the direct displacement-based seismic design (DBSD) method is becoming accepted throughout the engineering community as an effective tool to design BRBFs (Kim and Seo 2004; Teran-Gilmore and Virto-Cambray 2009). However, the damage caused by earthquakes is closely related to the structural cumulative hysteretic energy, which is not considered in the DBSD method (Bojórquez et al. 2011). In recent years, some researchers have used energy methods to measure the damage state of structures (Wong and Yang 2001; Bojórquez et al. 2010). Consequently, as an alternative design method to SBSD and DBSD, energy-based seismic design (EBSO) methods (Housner 1956; Akiyama 1985; Uang and Bertero 1990) have increasingly been used in the design of BRBFs (Choi and Kim 2006; Sahoo and Chao 2010; Khampanit et al. 2014). EBSO is mainly focused on the mitigation or control of damage in primary structural systems under different performance levels. One of the key design aspects of EBSO is to determine the distribution of the hysteretic energy demand within stories and even for all structural components (Surahman 2007). For the BRBF, maximizing the proportions of the hysteretic energy distributed on the BRBs in the structure during severe future earthquake is one of the best energy dissipation mechanisms that EBSO aims to design. From this standpoint, structural optimization is believed to be a meaningful tool to achieve this goal.

With the development of structural optimization technology, the process of PBSO is moving towards that of automatic performance-based optimum seismic design (PBOSD) (Ganzerli et al. 2000; Fragiadakis et al. 2006; Liu et al. 2013, 2014). The majority of PBOSD process for an energy-absorbing structure belong to sequential pattern, which is characterized by first conducting the design of the main frames and then designing additional energy dissipation devices (FEMA 273 1997). However, these sequential designs cannot readily accommodate the coupling between the main frame and the energy dissipation devices and probably lose the best design (Haftka 1990; Soong and Cimellaro 2009). Recently several researchers have adopted collaborative optimal design for energy-absorbing structure in PBOSD (Gilbert and Schmidt 1991; Castaldo and De Iuliis 2014; Curadelli and Amani 2014). Their studies found that the collaborative optimal design could take the coupling behavior of two parts into consideration and produce global optimal designs. Unfortunately, most of the studies include only strength and deformation constraints, and few studies have focused on the BRB frame structures despite the fact that the introduction of BRBs inevitably affects the redistribution of the internal forces of structures. Some design requirements that are satisfied by original structures may be violated by the introduction of BRBs.

The collaborative optimal design of BRBFs, as most PBOSD problems, contains both continuous and discrete variables, with non-linear performance objectives and design

requirements, which can be formulated as non-convex Mixed-Integer Non-Linear Programming (MINLP) problems. Basically, MINLP solvers can be categorized into two types: deterministic and non-deterministic (Zhou et al. 2014). During the past decades, a number of deterministic methods have been proposed to solve convex MINLPs (Geoffrion 1972; Gupta and Ravindran 1985; Westerlund and Pettersson 1995). However, to solve the non-convex MINLPs, many of these algorithms assume convexity of the search space and may cut off the global optimum solution. In addition, they suffer from the curse of dimensionality, wherein there is an exponential increase in the calculation cost for a linear increase in the problem size. In recent years, the non-deterministic algorithms, with the advantage of seeking the global optimal solution and requiring no derivative information of problem formulation, have attracted wide attention to solve non-convex MINLPs, such as genetic algorithm (GA) (Cheung et al. 1997), simulated annealing (SA) (Cardoso et al. 1997), and ant colony optimization (ACO) (Schluter et al. 2009). However, most of the aforementioned approaches are designed for single-objective MINLP, and few attempts have been made to develop and extend to multi-objective MINLP (MO-MINLP) so far.

This paper presents a collaborative optimization design method for buckling-restrained braces and steel frames in the framework of PBSO. In the optimization process, the design specifications and engineering requirements are comprehensively considered, including the geometric constraints, conceptual design constraints, strength requirements, stability requirements, displacement limitations, and ductility constraints. The purpose of the optimal design is to minimize the cost of structural initial materials while maximizing the story energy dissipation ratio of BRBs under major earthquakes. A modified hybrid coding non-dominated sorting genetic algorithm II (NSGA-II) (Deb et al. 2002) is used to perform multi-objective collaborative optimization design for structures including discrete steel frame design variables and continuous BRB design variables. A seven-story BRB steel frame structure is used to verify the rationality of the proposed optimization procedure, and three typical design schemes in the Pareto optimal set are selected for performance evaluation and comparison.

2 Performance-based energy dissipation analysis of BRBFs

2.1 Performance objective requirements

A performance objective is defined as a desired target performance level that corresponds to a specific hazard level. The most commonly used three performance levels recommended by the FEMA 273 report (1997), i.e., immediate occupancy

(IO), life safety (LS), and collapse prevention (CP), are adopted, which have been reflected in the Chinese design codes (GB50011 2010; GB50017 2017). In the case of BRBFs, under frequent-level earthquakes, BRBs mainly contribute a large portion of the lateral stiffness to the BRBFs to help the steel frames (i.e., primary structure) maintain elastic. As the first earthquake fortification line in dual structural systems, BRBs are intended to yield prior to the steel frames and dissipate a major portion of the hysteretic energy under moderate-level earthquakes. In this case, the steel frames can be repairable, and the BRBs can be replaced easily in the manner of a fuse. When excited with rare-level earthquakes, BRBs are still designed to dissipate a significant portion of the total hysteretic energy and can control the damage development in the steel frames for structural safety. For these purposes, two key issues should be seriously treated in the multi-objective collaborative optimization process. One is to ensure that yielding of BRBs occurs before that of the steel frame. The other is to maximize the proportion of energy dissipated by BRBs under rare-level earthquakes.

2.2 Pushover analysis

To ensure computational efficiency and to achieve motion-independent results during the optimization, the widely used incremental static analysis procedure, i.e., the pushover analysis method recommended by FEMA 356 (2000), is applied. It has been demonstrated that if the structural earthquake response is dominated by the fundamental vibration, the results from the pushover analysis can desirably capture the damage development within the structural components as the earthquake intensity increases (Krawinkler 1995). Usually, the displacement control pattern based on the fundamental mode of a structure of concern is maintained throughout the pushover analysis until structural failure is declared. The results from the pushover analysis are expressed as the relation curve between the base shear, V_b , and the roof displacement, δ_f . The key to the pushover analysis method used in PBSO lies in the determination of the target roof displacement δ_t of a structure under a specific performance level. The capacity spectrum method (Fajfar 1999) and the displacement coefficient (FEMA 273 1997) method can be used to obtain the target roof displacement δ_t . From the standpoint of computerized implementation, the latter is adopted, i.e.,

$$\delta_t = C_0 C_1 C_2 C_3 S_a \frac{T_c^2}{4\pi^2} g \quad (1)$$

where C_0 , C_1 , C_2 , are C_3 are the modification factors defined in FEMA 356; g is the gravity acceleration; and S_a is the spectral acceleration at the fundamental period, T_c . As suggested by FEMA 273 (1997), T_c is determined by the effective elastic stiffness of a bi-linearized pushover curve. As the

determination of the target displacement is related to the bi-linearization of the pushover curve, some iteration may be required.

2.3 Structural fuse

Figure 1 schematically illustrates the piecewise force (V) vs. story drift (Δ) relation curves of the BRBs, steel frame, and BRBFs. To ensure that the BRBs can successfully play the role of a structural fuse in the dual structural system of BRBFs, the BRBs at any story are designed to yield before the frame part at that story (Vargas Bruneau 2009), i.e.,

$$\Delta_F > \Delta_{BRB} \quad (2)$$

where Δ_F and Δ_{BRB} are the yield story drifts of the steel frame and BRBs, respectively. Note that the determination of Δ_{BRB} is related to the material properties and the inclination of the BRBs, independent of cross-sectional area of the steel core (Kim and Seo 2004). Low yield point steel, which has a relatively low yield strength and excellent energy dissipation capacity, is preferred for the steel core of BRBs.

2.4 BRB energy dissipation ratio

During the vibration of structures, the earthquake input energy is converted into kinematic energy, viscous damping energy, elastic strain energy, and plastic hysteretic energy. From the standpoint of EBSD methodology, only the hysteretic energy can cause structural damage when an earthquake terminates. The structural damage can be well controlled by suitable distribution of the hysteretic energy dissipated within the structural components (Habibi et al. 2013). In BRBFs, the BRBs can dissipate a substantial portion of the hysteretic energy through the plastic yielding of the steel core to mitigate the damage accumulated in the steel frame components (Sahoo and Chao 2010). To characterize the involvement of the BRBs in hysteretic energy dissipation in the whole system, the BRB

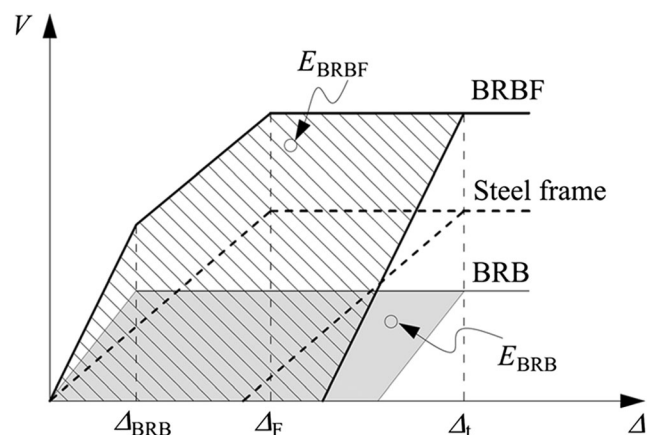


Fig. 1 Schematic illustration of idealized force vs. displacement curves of BRBF

energy dissipation ratio in the whole system, R , is defined to describe the system-level energy dissipation efficiency of the BRBs, i.e.,

$$R = \frac{\sum_{i=1}^{ns} E_{BRB}^i}{\sum_{i=1}^{ns} E_{BRBF}^i} \quad (3)$$

where ns is the number of stories, E_{BRB}^i is the hysteretic energy dissipated in the i th story by the BRBs, and E_{BRBF}^i is the hysteretic energy dissipated in the i th story of the BRBF (see Fig. 1). It can be seen from (3) that the energy dissipation role of BRBs in the whole system can be roughly enhanced by increasing the value of R . However, considering the possibility of weaker stories, the participation of BRBs in hysteretic energy dissipation in all stories cannot be guaranteed by simply maximizing the system-level BRB energy dissipation ratio. Therefore, to characterize the involvement of the BRBs in the hysteretic energy dissipation within a specific story, the so-called BRB energy dissipation ratio of the i th story, r^i , is introduced and defined as follows:

$$r^i = \frac{E_{BRB}^i}{E_{BRBF}^i} \quad (4)$$

Akiyama (1985) believed that the hysteretic energy dissipation of an inelastic structural system is dominated by its fundamental vibration mode. Therefore, the story shear vs. story drift response curve (see the shadowed area in Fig. 1) obtained from the pushover analysis can be used to determine the BRB energy dissipation ratios of all stories under the performance levels of interest. It is noted that the irreversible elastic strain energy should be excluded in the calculation of BRB energy dissipation ratios.

3 Collaborative optimum design of BRBFs

3.1 Discrete-continuous hybrid design variables

For the sake of simplicity, only the optimization on the cross-section of both frame components and BRBs is concerned in the proposed collaborative optimization method. The other design factors, e.g., structural layout, material properties, and BRB configuration, are not included and assumed to be determined prior to the optimization. The variation of the placement of BRBs along structural height, i.e., topology optimization, is reflected indirectly though broadening the range of BRB parameters during the optimization.

In most cases, the cross-sections of the steel columns and beams are selected from the section list provided by commercial design software or manufacturer, e.g., AISC 341 (2016). The series numbers of the sections in these databases can be included in the design profile list and treated as possible

values of the section design variables of the columns and beams. Thus, the optimization of the section of frame columns and beams is a typical integer program problem, i.e., a discrete optimum problem. Although some models of BRBs are available for designers, there is still a great demand for customized products from users because seismic retrofitting using BRBs is strongly dependent on the behavior of the structure under concern. Among all the parameters associated with BRBs as shown in Fig. 2, the area and yield strength of the steel core segment where the dissipated hysteretic energy is concentrated are the most dominant. These parameters mostly control the stiffness and strength of the BRBs, respectively. Since only a few kinds of steel materials, e.g., low yield point steel, are used in BRBs, it is reasonably acceptable to take the area of steel core segment as a main continuous control parameter in the optimization. As illustrated in Fig. 2, the core plate of a BRB generally consists of two elastic connection segments and two constrained transition segments at its ends, as well as a core segment. For analytical convenience, a truss element with a constant section equal to that of the core segment is usually applied to simulate the behavior of the BRB (Tsai and Hsiao 2008). The equivalent axial stiffness and modulus of elasticity, i.e., K_{eff} and E_{eff} , can be determined by.

$$K_{\text{eff}} = E_b \frac{A_c A_k A_t}{L_k A_c A_t + L_t A_c A_k + L_c A_k A_t} \quad (5a)$$

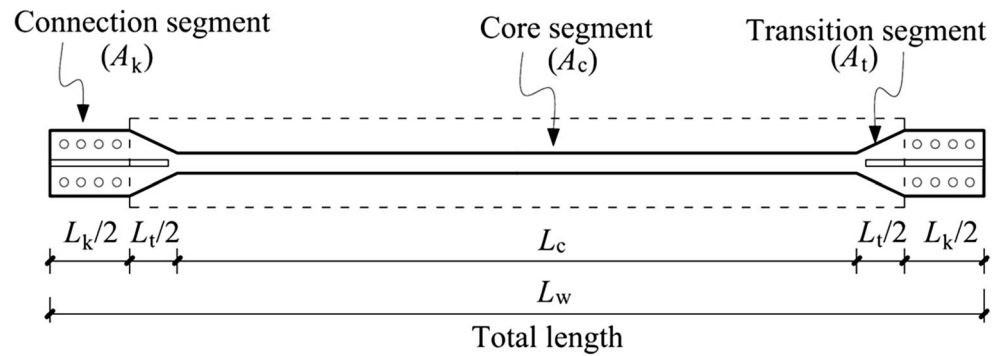
$$E_{\text{eff}} = K_{\text{eff}} \frac{L_w}{A_c} = E_b \frac{L_w A_k A_t}{L_k A_c A_t + L_t A_c A_k + L_c A_k A_t} \quad (5b)$$

where E_b is the modulus of elasticity of the steel core segment. The definitions of the other geometrical parameters can be seen in Fig. 2. All these parameters of BRB can be regarded as continuous variables. This gives the problem its continuous feature. As a result, two types of design variables, i.e., the continuous variables of BRBs and the discrete variables of frame components (columns and beams), will be treated in the optimization process.

3.2 Constraints

Any rational scheme of BRBFs should comply with some certain geometrical and conceptual design constraints. To make the variation in lateral stiffness along structural height be more reasonable, the area of a column located in the upper stories should be less than that located in the lower stories. To facilitate the detailed design of beam-column joints, the width of the flange of a steel beam should not be greater than that of the connected columns. To form a rational energy dissipation mechanism, the structural fuse requirements of BRBs in Section 2.3 are also taken as constraints here. In addition, at any beam-column joint, the sum of the plastic bending moments of the connected columns is required to be larger than that of the

Fig. 2 Details of a BRB component



connected beams in order to guarantee the ductile strong-column-weak-beam mechanism (AISC 341 2016; GB50017 2017). In this case, the beams are intended to yield before the columns. It is particularly meaningful to avoid possible unfavorable progressive collapse patterns of structures under strong earthquakes.

The check on the requirement of strength and stability should be carried out during the first design stage (GB50017 2017), e.g., the capacity of the compression-bending columns, the local and global stability of the beams and columns, the flexural and shear capacity of the beams, and the axial capacity of the BRBs. Two load effect combinations are included, i.e., the typical non-seismic design combination of $1.35D + 0.7 \times 1.4 L$ and the typical seismic design combination of $1.2(D + 0.5 L) + 1.3E$, where D , L , and E represent the dead load, live load, and earthquake action, respectively. The modal decomposition method combined with the code-specified response spectrum (GB50011 2010) is applied to determine the earthquake response.

Structures that satisfy the abovementioned requirements on strength and stability are also required to satisfy the constraints of the deformability limits of structures corresponding to different performance levels. The story drift limits of 0.5%, 1.5%, and 2% are suggested in FEMA 356 (2000) for the IO, LS, and CP performance levels, respectively. BRBs are intended to yield but not fail under the LS and CP performance levels. As recommended by Usami et al. (2003), the maximum deformation ductility factor of the BRBs should not be greater than the allowable limit of 25 for both compression and tension.

3.3 Objective functions

The first goal of this work is to properly distribute the hysteretic energy dissipated by the whole system. The proposed energy dissipation ratio is used to act as an indicator to measure the performance of the energy distribution mechanism. In other words, to achieve a rational energy distribution mechanism is to maximize the BRB energy dissipation ratio at each story and to minimize the involvement of the steel frame components in the dissipation of hysteretic energy. To fulfill this

purpose, the minimum of all story BRB energy dissipation ratios is controlled in the collaborative optimization.

$$\text{Minimize : } f_1 = \max\{1-r^1, 1-r^2, \dots, 1-r^i, \dots, 1-r^N\} \quad (6)$$

where f_1 is the maximum of the frame energy dissipation ratios, r^i is the energy dissipation ratio in the i th story, and N is the number of stories. Note that controlling the total value of the structural hysteretic energy is not the main goal of this work since this total value does not vary too excessively within feasible structures that meet the conceptual requirements, design specifications, and performance design requirements (the constraints of optimization) when the design conditions, geometric dimensions, and main component topologies are fixed.

As usual, the second objective is to minimize the total material cost, including the cost of the steel beams, columns, and BRBs. The material cost of the steel beams and columns, which are directly selected from some databases, can be easily determined by the product of the total steel amount used and the unit market price. As far as BRBs are concerned, they are generally priced in terms of a cost coefficient. Thus, the total material cost of a BRBF, f_2 , can be expressed as the following:

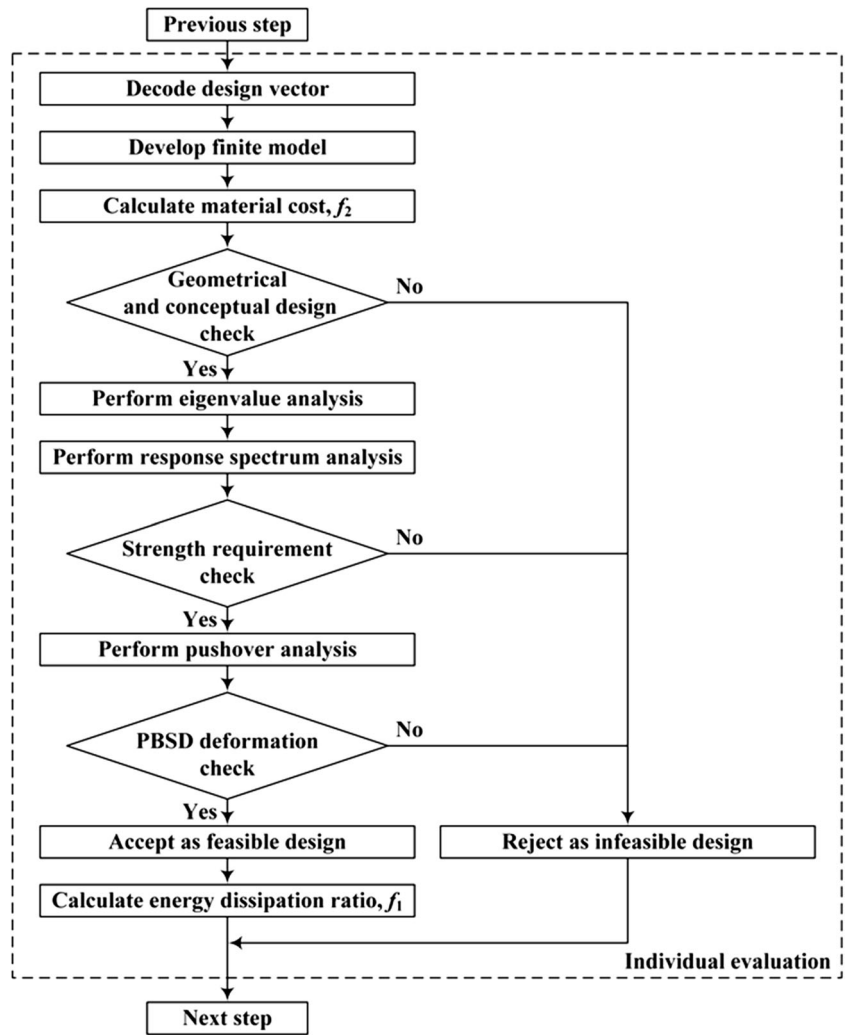
$$\text{Minimize : } f_2 = \omega_{bc} \sum_{i=1}^{n_{bc}} \rho_{bc} L_i A_i + \omega_{brb} \sum_{j=1}^{n_{brb}} \rho_{brb} L_{wj} A_{c_j} \quad (7)$$

where ω_{bc} and ω_{brb} are the market price of the steel components and BRBs, respectively; ρ_{bc} and ρ_{brb} are the density of the steel components and BRBs, respectively; n_{bc} and n_{brb} are the number of beam-column elements and BRB elements, respectively; L_i and L_{wj} are the length of the i th beam-column element and the j th BRB element, respectively; and A_i is the area of the i th beam-column element. It is a discrete variable; A_{c_j} is the area of the j th BRB element. It is a continuous variable.

3.4 Formulation of optimization problem

The problem of the performance-based collaborative optimization design of BRBFs contains nc real value design variables for the BRB parameters and nd integer value design variables for the cross-section of steel beams and columns.

Fig. 3 Individual evaluation



The optimization objective functions include the material cost and the maximum story energy dissipation ratio of the steel frame. As discussed previously, the constraints consist of those from geometrical and conceptual design requirements, strength and stability requirements, and deformation checks within the PBSD framework. Thus, the collaborative optimization formulation of BRBFs falls into the category of problems known as multi-objective Mix-Integer Non-Linear Program (MO-MINLP) problems, as expressed by

Find : $\{C, D\}$

$$= \{c_1, c_2, \dots, c_i, \dots, c_{nc}, d_1, d_2, \dots, d_j, \dots, d_{nd}\}^T \quad (8)$$

To minimize : $f_1(C, D), f_2(C, D) \quad (9)$

Subject to : $g_l(C, D) \leq 0 \quad l = 1, 2, \dots, ng \quad (10)$

where c_i is the value of the i th real value continuous design variable of the BRBs ($i = 1, 2, 3, \dots, nc$) and d_j is the value of

the i th integer value discrete design variable of the beams and columns ($j = 1, 2, 3, \dots, nd$). C and D are continuous and discrete design variable vectors, respectively, with $C = \{c_1, c_2, \dots, c_i, \dots, c_{nc}\}$ and $D = \{d_1, d_2, \dots, d_j, \dots, d_{nd}\}$; g_l is the l th constraint; and ng is the number of constraints.

The main contribution of the problem formulation in this work is that the proposed collaborative optimal design framework for BRBFs, in which the frame components and the BRBs are simultaneously treated as design variables, considers three performance requirements of BRBF structure corresponding to three hazard-level earthquakes and containing the constraints to ensure that the BRBs work as energy fuses. In addition, the energy dissipation ratio objective is introduced to ensure that major damage is confined to the replaceable BRBs. Note that the constraints in this formulation include the principles of SBS and DBSD as mentioned previously, while the concept of EBSD is considered through introducing the energy-dissipated ratio in the objective

function. That is, SBS and DBSD requirements are strong conditions that any feasible designs must satisfy, and the EBSD concept is an additional condition that is used to improve the performance of the structure.

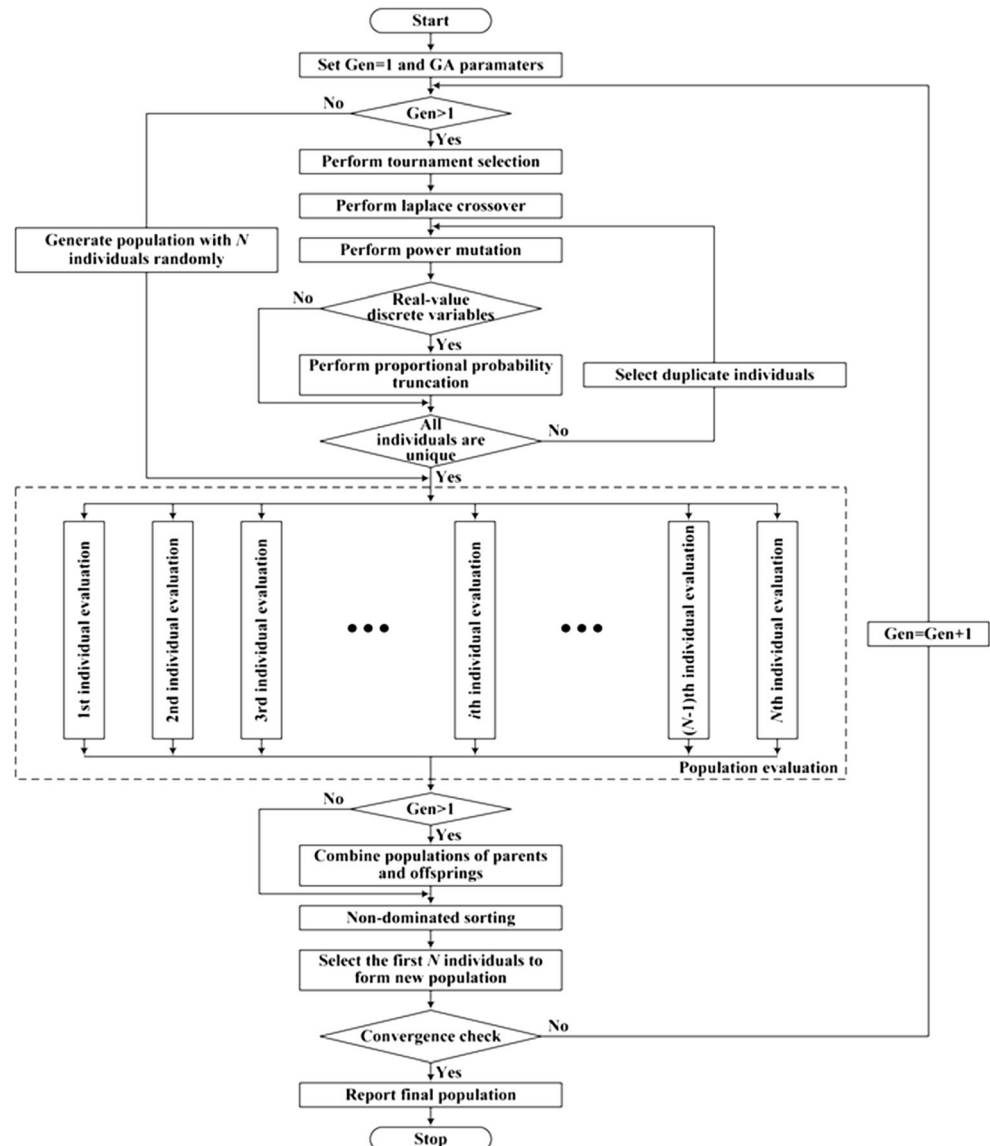
In the optimization process, each individual needs to be evaluated to calculate the values of the two objective functions. All the constraints should be satisfied before the generation of a feasible design. Figure 3 shows the procedures of the individual evaluation. The OpenSees program developed by the Pacific Earthquake Engineering Research (PEER) Center (2016) is used to establish finite element models and to perform response spectrum analysis and pushover analysis. The framework of the optimization problem is coded with Tcl script language, which is able to be seamlessly integrated with OpenSees.

4 Solution of multi-objective optimization problem

4.1 Hybrid coding NSGA-II

Among the abovementioned stochastic algorithm, the GA has received most attention from researchers due to its robust convergence and easy implementation compared with those of other methods. The most classic multi-objective version of GA, non-dominated sorting genetic algorithm II (NSGA-II) (Deb et al. 2002), is selected as the basis method to solve the multi-objective optimization (MOO) problem here mainly because of its proven capability in converging near the true Pareto optimal set while guaranteeing a diversity-preserving mechanism (Deb et al. 2002;

Fig. 4 Proposed optimization framework of BRBFs



Atamturktur et al. 2015). The original form of real-coded NSGA-II (Deb et al. 2002) applies binary crossover (SBX) and polynomial mutation operators, which are usually used to solve problems with continuous real value design variables. When the algorithm is applied to the case of discrete integer value design variables, two alternative modifications are available. One is to use binary encoding, while the other uses rounded-off real variables to address the integer restriction of decision variables. As a result of the Haiming Cliff (Herrera et al. 1998), the former modification will likely override the global optimal solution. For the latter, some identical results are likely to be generated during genetic operations. The randomness of the GA may be reduced. Recently, the Laplace crossover (LX) (Deep and Thakur 2007a) and the power mutation (PM) (Deep and Thakur 2007b) have been introduced into single-objective GA and exhibit superior efficiency in solving MINLP problems compared with other algorithms available in the literature (Deep et al. 2009).

To solve the MO-MINLP problem presented in this work, LX and PM are adopted into NSGA-II, which is then called the NSGA-II-LXPM. To be consistent with the hybrid coding scheme, the operations of crossover and mutation are performed simultaneously both in the discrete integer value design variables and the continuous real value design variables.

The parameterless method proposed by Deb et al. (2002) is used to deal with constraints during optimization, in which the effect of the degree of constraint violation during multiple-objective non-dominated sorting is considered. If a feasible

solution is compared with an infeasible solution, the feasible solution dominates. If both solutions are feasible, the dominant one is determined by the principle of multi-objective domination. If none of the solutions is feasible, the solution with a lower degree of violation is preferred. By the constraint handling method, the probability of the infeasible solutions in the population being selected for crossover operation is reduced gradually. Thus, the infeasible solutions in the population move closer to the feasible domain. It is noteworthy that finite element analysis is not required when handling the constraints from the abovementioned geometrical and conceptual design rules. To reduce unnecessary computational workload for achieving higher efficiency, the population is confined to those individuals satisfying these rules after the operations of crossover and mutation.

4.2 Proportional probability truncation operator and duplicate check operator

It is noteworthy that after the operations of crossover and mutation, the genes encoded by the integers in a chromosome can possibly generate non-integer gene values. It is necessary to deal with this aspect before decoding the genes into the space of design variables. Thus, a proportional probability truncation operator is proposed as follows,

$$x'_i = \begin{cases} \text{int}(x_i) & 0 \leq w_i < \gamma \\ \text{int}(x_i) + 1 & w_i \geq \gamma \end{cases} \quad (11)$$

where x_i is the non-integer value generated after the crossover and mutation operations for the genes encoded by integers; x'_i is the truncated value of x_i ; γ is a random number following the uniform distribution in the range of [0, 1]; and w_i is the decimal part of x_i , $w_i = x_i - \text{int}(x_i)$. The probability of rounding up (or down) is equal to the decimal part of the non-integer value, w_i . Such truncation operation can not only relate it to the original gene value but also introduce some randomness in the genes to avoid repetitive generations of identical integer values.

Unlike the case of SOO, there is a specific goal in a MOO in addition to convergence to the optimal design (Pareto optimal set for MOO): maintenance of diversity in solutions of the Pareto optimal set. For the real-coded GA, after the operations of selection, crossover and mutation, the offspring that have identical chromosomes are produced inevitably with a certain probability. In a MOO case, these two identical individuals overlap each other in the space of the objective function. We require the optimizer to find a set of solutions that are non-dominated and are widely spread over the approximated Pareto front. Excessive overlapping individuals are

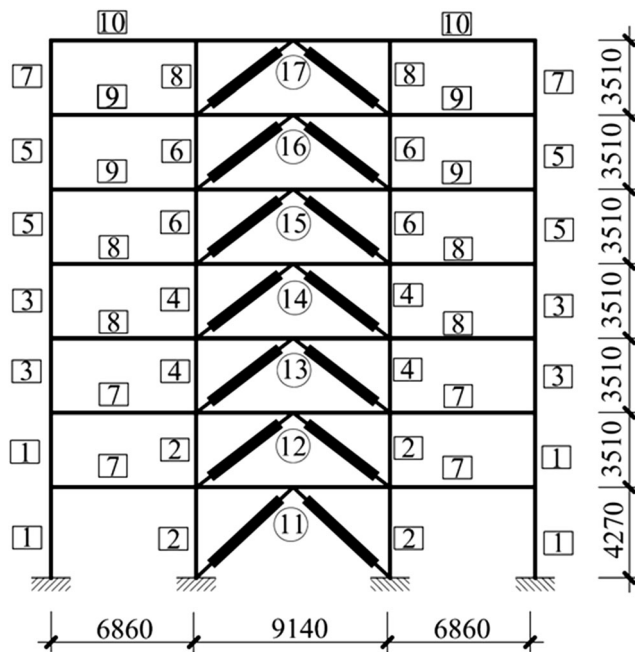


Fig. 5 A seven-story steel BRBF (units: mm)

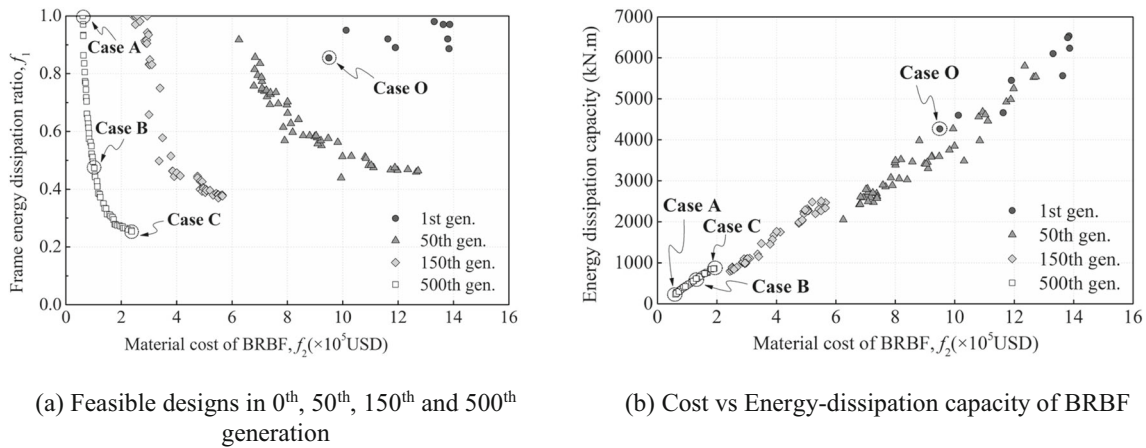


Fig. 6 Converge history of modified NSGA-II-LXPM. **a** Feasible designs in 0th, 50th, 150th, and 500th generation. **b** Cost vs. energy dissipation capacity of BRBF

detrimental to the continuity and diversity of the Pareto front. It can also make the algorithm be premature during the iteration. To solve this issue, the method proposed by Mauldin (1984) is applied to record the values of the chromosomes of all individuals and to conduct a duplicate check operator in population. The forced mutation is performed for the duplicate of populations in order to create different individuals. Such operator can improve the convergence rate and maintain the diversity of populations. Figure 4 illustrates the flowchart of the proposed optimization method with the modified NSGA-II-LXPM.

4.3 Optimal decision-making scheme

The convergence to an absolute optimum solution is not an inherent property of a multi-objective evolutionary algorithm, but it is still possible to introduce some specific conditions to stop the algorithm. In this research, the algorithm is assumed to converge to a set of Pareto optimal solutions when it has evolved prespecified maximum number iterations.

The optimal solutions of the multi-objective optimization problem form a Pareto set in which none of the solutions have a dominant relation between each other. A decision-maker should adopt a preference function to choose an ideal solution from all the alternatives in the set. In design practice, after a Pareto optimal curve is obtained, some representative optimal solutions can be considered for final performance assessment.

As far as the collaborative multi-objective optimization problem is concerned, three cases can be considered, i.e., (1) case A: the optimal solution having the minimum value of the 1st objective function; (2) case C: the optimal solution having the minimum value of the 2nd objective function; and (3) case B: the optimal solution having the shortest Euclidean distance to the origin, as determined by Deb and Sundar (2006).

5 Application

5.1 Basic information

Figure 5 shows a seven-story steel BRBF designed in accordance with current Chinese codes (GB50011 2010; GB50017 2017) with a precautionary intensity of 8° (design PGA = 0.20 g), the first seismic design group, and the site classification of the I-category. The numbers in the rectangular boxes represent the group numbers of ten discrete variables, while those in the circles represent the group numbers of seven continuous variables. A gravity load is applied on the beams in terms of uniform distribution loads. The design floor dead and floor live loads are 4.16 kN/m² and 2.82 kN/m², respectively. The design roof dead and roof live loads are 2.39 kN/m² and 0.958 kN/m², respectively. The AISC 341 (2016) section list is used for the selection of the beams (from 238 I-type sections) and columns (from 39 W14 sections). The yield strength of all the beams and columns is 344.74 MPa. The

Table 1 Values of the optimal objective function of five solutions

Minimum objectives	Solutions				
	1st solution	2nd solution	3rd solution	4th solution	5th solution
f_1^{\min}	0.271	0.254	0.268	0.269	0.289
f_2^{\min}	61154	60279	65954	63274	61373

Table 2 Some information of case A, case B, case C, and case O

Design variables		Cases			
		Case A	Case B	Case C	Case O
Column	1	W14 × 120	W14 × 90	W14 × 53	W14 × 873
	2	W14 × 53	W14 × 61	W14 × 82	W14 × 455
	3	W14 × 74	W14 × 43	W14 × 48	W14 × 873
	4	W14 × 53	W14 × 53	W14 × 82	W14 × 398
	5	W14 × 38	W14 × 43	W14 × 48	W14 × 257
	6	W14 × 43	W14 × 43	W14 × 38	W14 × 398
	7	W14 × 38	W14 × 43	W14 × 48	W14 × 257
	8	W14 × 43	W14 × 43	W14 × 38	W14 × 398
Beam	9	W16 × 40	W16 × 36	W16 × 40	W27 × 178
	10	W18 × 35	W16 × 31	W16 × 31	W27 × 129
	11	W16 × 31	W16 × 31	W16 × 31	W24 × 55
Brace (cm ²)	12	W16 × 26	W16 × 26	W16 × 31	W27 × 94
	13	5.4032	21.0600	58.2332	216.4029611
	14	4.4092	20.2601	46.4098	242.2029611
	15	4.4079	21.9423	45.0201	222.8529611
	16	1.7248	14.6330	38.6200	177.4039653
	17	0	11.1528	26.2934	183.8539653
	18	0	7.69276	18.5696	94.10055642
	19	0	4.51000	12.9943	148.2805564
Objective function	f_1	1.0	0.4509	0.2538	0.8543
	f_2 (USD)	60279	97546	237503	949941

area of the core part of the BRBs varies from 0 (i.e., with no BRB core) to 64,516 mm², with the yield strength of 317.16 MPa.

All the analytical models are established by the OpenSees program in which the beams and BRBs are modeled by the non-linear beam-column elements and the CorotTruss element, respectively, with the same Steel02 material. The cross-section of the core part of the BRBs is taken as that of the CorotTruss element, and the equivalent modulus of elasticity is determined by Equation (5). The damping ratio is assumed to be 2%. In view of the rigidity of the connection steel plates, all the beams are assumed to be rigidly connected with the columns, while the BRBs are pin-connected with the beam-column joints. In addition, the diaphragm is assumed to be in-plane rigid. As mentioned previously, the limits of story drift of the BRBF under the IO, LS, and CP performance levels are 0.5%, 1.5%, and 2% (FEMA 356 2000). During the optimization process, the response of all elements in each generation is stored in the memory to obtain the structural global response. The stored response data of the elements is released from the memory if the computation of the objective functions and constraint functions is accomplished.

The parameters for the algorithm are as follows: the scale of the population is 50, and the scale of the tournament is 2; the maximum number of iteration is 500; the crossover probability is 0.95; the mutation probability is 0.01. The

configurations of the BRBs are selected from Tsai and Hsiao (2008), where the ratios of the section of the connection segment and transition segments to that of core segment are $A_k/A_c = 2.2$ and $A_t/A_c = 1.6$, respectively. The normalized lengths of the connection segment, transition segment, and core segment with respect to the total specimen are $L_k/L_w = 0.24$, $L_t/L_w = 0.06$, and $L_c/L_w = 0.70$. The material cost of the steel frame is evaluated by the density of steel of $\rho_{bc} = 7850$ kg/m³ and a price of $\omega_{bc} = 3$ USD/kg. The material cost of the BRBs is calculated based on the density of the BRBs of $\rho_{brb} = 46800$ kg/m³ and a price of $\omega_{brb} = 9$ USD/kg.

5.2 Results and discussion

As a population-based optimization algorithm, the efficiency of the proposed method is highly dependent on the first generation. At the beginning of optimization, an initial population with a scale of 50 is randomly generated, and only one, 2% of the population size, is proven to be feasible after checking an enormous amount of constraint satisfaction statuses, which seriously affects the efficiency of the optimization. To this end, the designs in the initial population are created with a restriction to satisfy all the geometrical and conceptual design rules before performing FEA. With this constraint reduction method, the proportion of feasible designs is increased to

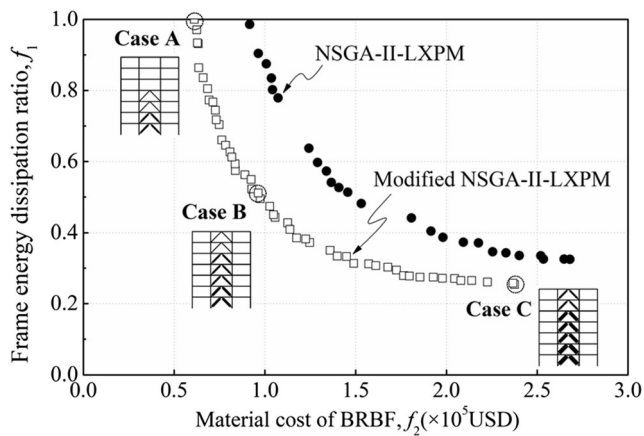


Fig. 7 Pareto front obtained by algorithms

almost 20%. Figure 6 a presents the nine feasible designs in the first generation, all designs in the 50th generation, 150th generation, and the Pareto front in the 500th generation. It can be seen that the population is converging to the Pareto front during optimization.

The pushover curves of all feasible designs in Fig.6a are obtained as the roof displacement reaches 3.0% of the total height of the structure. The energy dissipation capacities, calculated from the pushover curve, are presented with the corresponding material costs in Fig.6b. The results indicate that the feasible designs that satisfy all the design requirements have an energy dissipation capacity that is proportional to their costs.

In view of the randomness of the GA, the algorithm has been tested five times with the parameters defined previously during the optimization process. Table 1 lists the values of the optimal objective function of the solutions. The differences among the values are insignificant, indicating the desirable stability of the modified NSGA-II-LXPM. Three cases located on the Pareto front of the last generation, i.e., case A, case B, and case C, are selected by the abovementioned decision-making scheme. In addition, among the nine feasible designs in the first generation, case O, the non-dominated design with

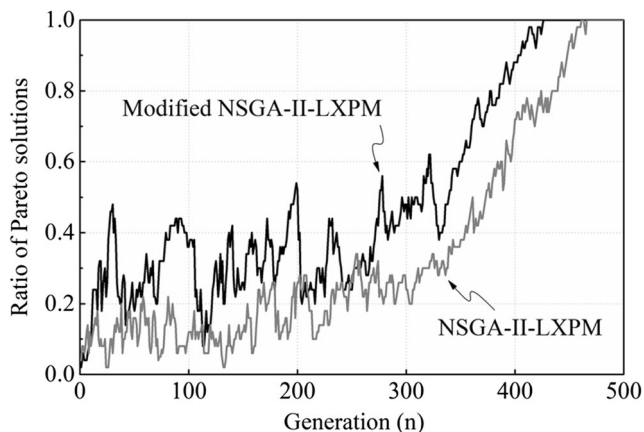


Fig. 8 Evolutionary process of Pareto solutions

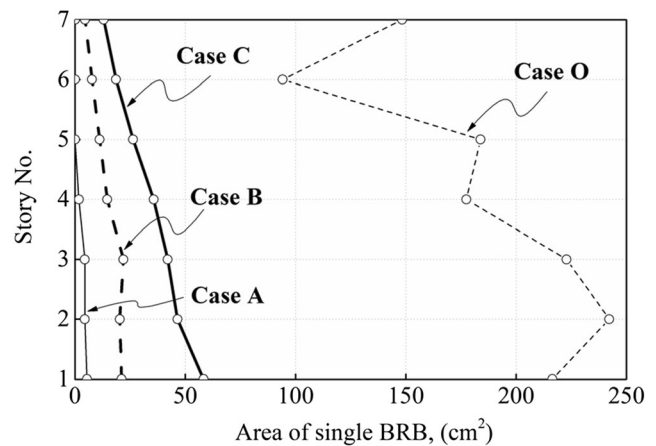
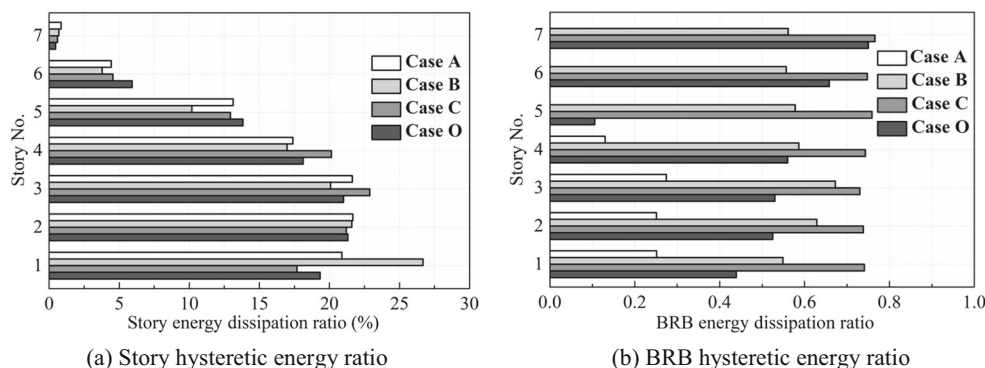


Fig. 9 Distribution of area of BRBs along height

the smallest values of both objective functions, is also selected. The four cases are presented in Fig.6a, and their values of the design variables and the objective functions are listed in Table 2. Case A has the lowest material cost; nevertheless, some stories of its primary structure are heavily involved in energy dissipation. The material cost of case B is 61.8% higher than that of case A. The BRBs in all stories can accommodate at least 55% of the story hysteretic energy dissipation. The material cost of case C is the highest on the Pareto front, nearly four times the cost of case A and 2.4 times that of case B. Case C has the largest BRB energy dissipation ratios among the three cases. The frame energy dissipation ratios are less than 0.24, which implies that the BRBs can dissipate up to 76% of the hysteretic energy dissipated by the corresponding story. However, even if the area of the BRBs increases further, the proportion of hysteretic energy absorbed by the BRBs shows no increase. That is because the frame may become weaker compared with the BRBs. In this case, the BRBs may yield later after the frames and lose their role as structural fuses, leading to an infeasible design.

The Pareto front formed by 50 optimal solutions after 500 generations is shown in Fig. 7. It is observed that the solutions can converge at a Pareto front with a smaller objective function, compared with NSGA-II-LXPM, by the modified NSGA-II-LXPM and that the diversity of optimal solutions is greatly enhanced. Figure 8 displays the evolution curve of the ratio of the Pareto solutions among the populations during optimization. The original algorithm demonstrates a moderate fluctuation, and all of the searching processes converge to the Pareto front at a relatively slow speed. In contrast, the curve of the modified NSGA-II-LXPM fluctuates apparently at the first half of the evolution process and increases steeply at the latter half, which indicates that the algorithm searches extensively when far away from the Pareto front and concentrates on searching for optimal designs when close to the front. Thus, as has been said, the modified NSGA-II-LXPM exhibits a

Fig. 10 Distribution of hysteretic energy dissipation. **a** Story hysteretic energy ratio. **b** BRB hysteretic energy ratio



higher efficiency in searching for the Pareto front and ensuring the diversity of the result solutions.

As illustrated by Fig. 9, the BRB areas of the randomly generated case O distribute irregularly; interestingly, the areas of the BRBs of all three cases on the Pareto front distribute almost linearly along the height. In addition, it can be observed that the placement of the BRBs in the lower stories of the frame is economically more efficient than in case A.

The distribution of the story hysteretic energy dissipation is illustrated in Fig. 10a. As shown in Fig. 10a, case A tends to have a relatively uniform distribution of the story hysteretic energy dissipation, while case B has an inversed triangular distribution pattern. The maximum story hysteretic energy dissipation of case C occurs at the third story. The proportion of hysteretic energy dissipated by the BRBs, in terms of the BRB energy dissipation ratio, is shown in Fig. 10b. The ratios of case C are uniformly distributed along the height, varying between 73 and 76%. In this case, the damage caused by strong earthquakes in the columns and beams can be substantially reduced. The ratio of energy dissipated by the BRBs in case O drops dramatically in the fifth story, revealing that case O has a larger coefficient of variation of the energy dissipation ratio.

The distributions of the story drifts of the four cases under IO, LS, and CP performance levels are illustrated in Fig. 11. Compared with the three optimal designs on the Pareto front, case O has a more conservative inter-story drift under all three performance levels, especially under the CP level. As

indicated by the proposed optimization method, the maximum story drifts of all three cases on the Pareto front are close to the limit of 2% under the CP performance level. For the other two performance levels, the code-specified limits are satisfied with some reserve, especially for the case of the LS performance level.

As plasticity is developed and concentrated mostly at the beam-column joints, only damage developed in those regions is considered and characterized by the modified Park-Ang model (Kunnath et al. 1992), for the index DI_{PA} . Figure 12 illustrates the damage development of case C under the three performance levels. At the IO level, all the components, including the BRBs, either do not experience damage or experience slight damage only, satisfying the performance objective under frequent earthquake. Under the LS level, all the beams except for those on the top story and the columns in the first story experience slight damage. The other columns remain elastic. All the BRBs except for those in the top story yield. As the intensity of the earthquake increases, the deflection curve of the frame changes from flexure type to shear-flexure type. Under the CP level, all BRBs yield and severe damage is observed in the bottom columns, whose damage indexes are greater than 0.60. Plasticity is mostly concentrated on the beams, especially for those in the lower four stories. The damage of the others is still relatively slight. The strong-column-weak-beam yield mechanism is achieved. It is demonstrated that uniform damage distribution along the height can make BRBFs more ductile.

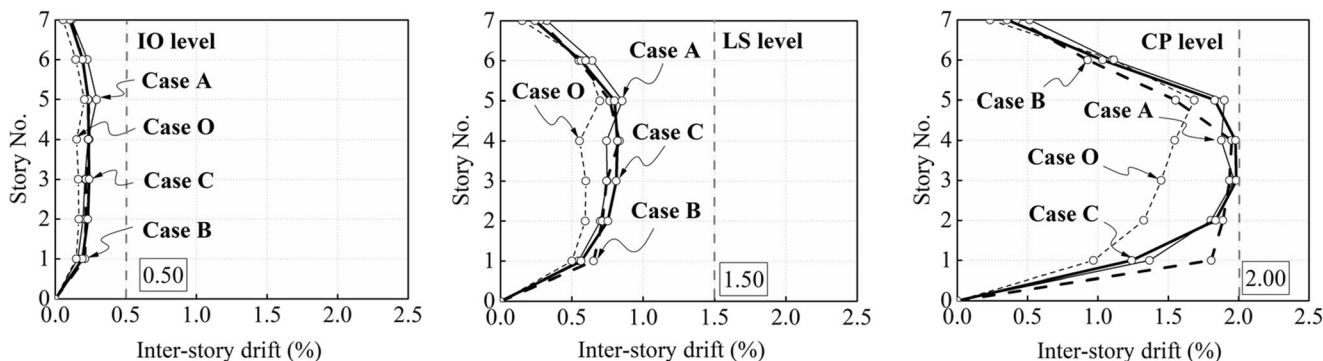
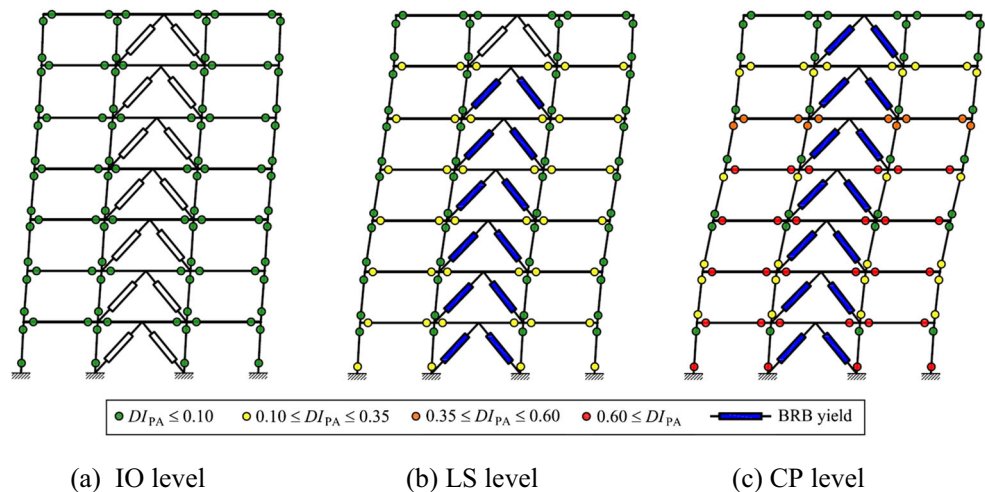


Fig. 11 Distribution of inter-story drift under different performance levels

Fig. 12 Distribution of plasticity in case C for three performance levels. **a** IO level. **b** LS level. **c** CP level



6 Conclusions

Within the framework of performance-based seismic design (PBSD), this paper presents a multi-objective collaborative optimization method for steel frames with buckling-restrained braces (BRBF) in order to minimize the damage of the primary structure, in which the NSGA-II algorithm is modified and the so-called BRB energy dissipation ratio is introduced. Based on the validation carried out on a planar seven-story steel frame with BRBs, some observations have been obtained as follows:

- (1) The proposed optimization method is effective for the achievement of the automatic design of steel BRBFs. The NSGA-II-LXPM can be applied to the simultaneous optimal design of steel frames with integer design variables for the columns and beams and continuous design variables for the BRBs. The proportional probability truncation operator and the duplicate check operator introduced can accelerate the convergence of the modified NSGA-II-LXPM and increase the diversity of the Pareto solutions. As multiple iterations can obtain close optimal solutions, the algorithm is proven to be repeatable and stable.
- (2) The consideration of the strength-related code provisions can make all structural components maintain their elasticity under frequent-level earthquakes. With structural fuse conceptual introduced as constraint in optimal designs, BRBs can yield before the frame components and work as fuses under moderate-level earthquakes, after which the strong-column-weak-beam yield mechanism can be well achieved. In the case of rare-level earthquakes, the damage can concentrate on the replaceable BRBs through the introduction of the energy dissipation ratio objective.

- (3) The results from the example steel frame indicate that the placement of BRBs in the lower stories is economically efficient. The feasible designs that satisfy all the design requirements have an energy dissipation capacity that is proportional to their costs, and BRBs installed in steel frames can dissipate up to 76% of the hysteretic energy dissipated by the corresponding story. The BRB areas of Pareto optimal designs vary almost linearly along the height of the stories. In addition, as the earthquake intensity increases, the deflection curve of the frame changes from the flexural shape to the shear-flexural shape; the inter-story drift limitations under major earthquakes are the active constraints compared with the minor and medium earthquakes. The desirable brace-beam-column damage evolution tendency is exhibited in the BRBFs designed with the proposed collaborative optimization framework.

7 Replication of results

The results presented in this article are produced based on the NSGA-II algorithm, finite element model build in OpenSees, and part of our in-house code in Tcl scripts. Code and data for producing the presented results will be made available upon request.

Funding information This research is financially supported by the National Natural Science Foundation of China (Grant No. 51878123).

Compliance with ethical standards

Conflict of interest The authors declare that they have no conflict of interest.

References

- Akiyama H (1985) Earthquake-resistant limit-state design for buildings. University of Tokyo Press, Tokyo
- American Institute of Steel Construction (2016) Seismic provisions for structural steel buildings. ANSI/AISC 341-16, Chicago
- Atamturktur S, Liu Z, Cogan S, Juang H (2015) Calibration of imprecise and inaccurate numerical models considering fidelity and robustness: a multi-objective optimization-based approach. *Struct Multidisc Optim* 51(3):659–671
- Bojórquez E, Reyes-Salazar A, Terán-Gilmore A, Ruiz SE (2010) Energy-based damage index for steel structures. *Steel Compos Struct* 10(4):331–348
- Bojórquez E, Terán-Gilmore A, Ruiz SE, Reyes-Salazar A (2011) Evaluation of structural reliability of steel frames: interstory drift versus plastic hysteretic energy. *Earthquake Spectra* 27(3):661–682
- Cardoso MF, Salcedo RL, de Azevedo SF, Barbosa D (1997) A simulated annealing approach to the solution of MINLP problems. *Comput Chem Eng* 21(12):1349–1364
- Castaldo P, De Iuliis M (2014) Optimal integrated seismic design of structural and viscoelastic bracing-damper systems. *Earthq Eng Struct Dyn* 43(12):1809–1827
- Cheung BKS, Langevin A, Delmaire H (1997) Coupling genetic algorithm with a grid search method to solve mixed integer nonlinear programming problems. *Comput Math Appl* 34(12):13–23
- Choi H, Kim J (2006) Energy-based seismic design of buckling-restrained braced frames using hysteretic energy spectrum. *Eng Struct* 28(2):304–311
- Curadelli O, Amani M (2014) Integrated structure-passive control design of linear structures under seismic excitations. *Eng Struct* 81:256–264
- Deb K, Sundar J (2006) Reference point based multi-objective optimization using evolutionary algorithms. In: *Proceedings of the 8th annual Conference on Genetic and Evolutionary Computation*, pp. 635–642
- Deb K, Agrawal S, Pratap A, Meyarivan T (2002) A fast and elitist multi-objective genetic algorithm: NSGA-II. *IEEE Trans Evol Comput* 6(2):182–197
- Deep K, Thakur M (2007a) A new crossover operator for real coded genetic algorithms. *Appl Math Comput* 188(1):895–911
- Deep K, Thakur M (2007b) A new mutation operator for real coded genetic algorithms. *Appl Math Comput* 193(1):211–230
- Deep K, Singh KP, Kansal ML, Mohan C (2009) A real coded genetic algorithm for solving integer and hybrid integer optimization problems. *Appl Math Comput* 212(2):505–518
- Fajfar P (1999) Capacity spectrum method based on inelastic demand spectrum. *Earthq Eng Struct Dyn* 28(8):979–993
- Federal Emergence Management Agency (1997) NEHRP guidelines for the seismic rehabilitation of buildings. FEMA 273, Washington, DC
- Federal Emergence Management Agency (2000) Prestandard and commentary for the seismic rehabilitation of buildings. FEMA 356, Washington, DC
- Fragiadakis M, Lagaros ND, Papadrakakis M (2006) Performance-based multiobjective optimum design of steel structures considering life-cycle cost. *Struct Multidisc Optim* 32.1:1
- Ganzerli S, Pantelides CP, Reaveley LD (2000) Performance-based design using structural optimization. *Earthq Eng Struct Dyn* 29(11):1677–1690
- Geoffrion AM (1972) Generalized benders decomposition. *J Optim Theory Appl* 10(4):237–260
- Gilbert MG, Schmidt DK (1991) Integrated structure/control law design by multilevel optimization. *J Guid Control Dyn* 14(5):1001–1007
- Gupta OK, Ravindran A (1985) Branch and bound experiments in convex nonlinear integer programming. *Manag Sci* 31(12):1533–1546
- Habibi A, Chan RW, Albermani F (2013) Energy-based design method for seismic retrofitting with passive energy dissipation systems. *Eng Struct* 46:77–86
- Haftka RT (1990) Integrated structure-control optimization of space structures. In: *Proceedings of the AIAA Dynamics Specialists Conference*, pp. 1–9
- Herrera F, Lozano M, Verdegay JL (1998) Tackling real-coded genetic algorithms: operators and tools for behavioural analysis. *Artif Intell Rev* 12(4):265–319
- Housner GW (1956) Limit design of structures to resist earthquakes. In: *Proceedings of the First World Conference on Earthquake Engineering*: 5:1–512
- Khampanit A, Leelataviwat S, Kochanin J, Warnitchai P (2014) Energy-based seismic strengthening design of non-ductile reinforced concrete frames using buckling-restrained braces. *Eng Struct* 81:110–122
- Kim J, Seo Y (2004) Seismic design of low-rise steel frames with buckling-restrained braces. *Eng Struct* 26(5):543–551
- Krawinkler H (1995) New trends in seismic design methodology. *Proceedings of the 10th European Conference on Earthquake Engineering*: 821–830
- Kunnath SK, Reinhorn AM, Lobo RF (1992) IDARC version 3.0: a program for the inelastic damage analysis of reinforced concrete structures. Technical report NCEER-92-0022. National Center for Earthquake Engineering Research, Buffalo
- Liu Z, Atamturktur S, Juang CH (2013) Performance based robust design optimization of steel moment resisting frames. *J Constr Steel Res* 89:165–174
- Liu Z, Atamturktur S, Juang CH (2014) Reliability based multi-objective robust design optimization of steel moment resisting frame considering spatial variability of connection parameters. *Eng Struct* 76(1):393–403
- Mauldin M (1984) Maintaining genetic diversity in genetic search. In: *Proceedings of the National Conference on Artificial Intelligence*: 247–250
- Ministry of Housing and Urban-Rural Development of the People's Republic of China (2010) Code for seismic design of buildings (GB50011–2010). China Architecture & Building Press, Beijing
- Ministry of Housing and Urban-Rural Development of the People's Republic of China (2017) Standard for design of steel structures (GB 50017-2017). China Architecture & Building Press, Beijing
- OpenSees version 2.5.0 (2016) Computer software. Pacific Earthquake Engineering Research Center, Berkeley, CA <http://opensees.berkeley.edu/>
- Sahoo DR, Chao SH (2010) Performance-based plastic design method for buckling-restrained braced frames. *Eng Struct* 32(9):2950–2958
- Schluter M, Egea JA, Banga JR (2009) Extended ant colony optimization for non-convex mixed integer nonlinear programming. *Comput Oper Res* 36(7):2217–2229
- Soong TT, Cimellaro GP (2009) Future directions in structural control. *Struct Control Health Monit* 16(1):7–16
- Surahman A (2007) Earthquake-resistant structural design through energy demand and capacity. *Earthq Eng Struct Dyn* 36(14):2099–2117
- Teran-Gilmore A, Virto-Cambray N (2009) Preliminary design of low-rise buildings stiffened with buckling-restrained braces by a displacement-based approach. *Earthquake Spectra* 25(1):185–211
- Tsai KC, Hsiao PC (2008) Pseudo-dynamic test of a full-scale CFT/BRB frame—Part II: Seismic performance of buckling-restrained braces and connections. *Earthq Eng Struct Dyn* 37(7):1099–1115
- Uang CM, Bertero VV (1990) Evaluation of seismic energy in structures. *Earthq Eng Struct Dyn* 19:77–90
- Uang CM, Nakashima M (2004) Steel buckling-restrained braced frames. In: Bozorgnia Y, Bertero VV (editors). *Earthquake engineering from engineering seismology to performance-based engineering*. CRC Press, Boca Raton (FL), [chapter 16]

- Usami T, Kasai A, Kato M (2003) Behavior of buckling-restrained brace members. Behavior of steel structures in seismic areas, In: Proceedings of the 4th international conference: 211–216
- Vargas R, Bruneau M (2009) Analytical response and design of buildings with metallic structural fuses. I. *J Struct Eng* 135(4):386–393
- Watanabe A, Hitomi Y, Seaki E, Wada A, Fujimoto M (1988) Properties of brace encased in buckling-restraining concrete and steel tube. In: Proceedings of the 9th World Conference on Earthquake Engineering: 719–724
- Westerlund T, Pettersson F (1995) An extended cutting plane method for solving convex MINLP problems. *Comput Chem Eng* 19:131–136
- Wong KK, Yang R (2001) Effectiveness of structural control based on control energy perspectives. *Earthq Eng Struct Dyn* 30(12):1747–1768
- Zhou K, Chen X, Shao Z, Wan W, Biegler LT (2014) Heterogeneous parallel method for mixed integer nonlinear programming. *Comput Chem Eng* 66:290–300

Publisher's note Springer Nature remains neutral with regard to jurisdictional claims in published maps and institutional affiliations.